

## Revisiting the emission behavior of the characteristic line $1s2p\ ^1P_1 \rightarrow 1s^2\ ^1S_0$ following electron-impact excitation of heliumlike ions

Z. W. Wu ,\* Z. Q. Tian, and C. Z. Dong

*Key Laboratory of Atomic and Molecular Physics and Functional Materials of Gansu Province, College of Physics and Electronic Engineering, Northwest Normal University, Lanzhou 730070, People's Republic of China*



(Received 5 October 2021; accepted 5 January 2022; published 20 January 2022)

In light of the work of Reed and Chen [*Phys. Rev. A* **48**, 3644 (1993)], electron-impact excitation from the ground state  $1s^2\ ^1S_0$  to the excited energy level  $1s2p\ ^1P_1$  of heliumlike ions and subsequent electric dipole radiative decay  $1s2p\ ^1P_1 \rightarrow 1s^2\ ^1S_0$  are revisited by using the multiconfigurational Dirac-Fock method and relativistic distorted-wave theory. Special attention is paid to the effect of the Breit interaction on the angular and polarization behaviors of the characteristic electric dipole line radiated from heliumlike ions. It is found that the presently obtained linear polarization without inclusion of the Breit interaction agrees very well with the results of Reed and Chen for all the heliumlike ions and impact electron energies considered. In contrast to the results of Reed and Chen, the Breit interaction makes the electric dipole line much less linearly polarized and anisotropic, especially for high- $Z$  ions and high impact energies. This behavior quickly becomes more prominent with increasing atomic number  $Z$  and impact energy.

DOI: [10.1103/PhysRevA.105.012815](https://doi.org/10.1103/PhysRevA.105.012815)

### I. INTRODUCTION

In 1993, Reed and Chen investigated the relativistic effects on linear polarization of characteristic photons emitted from the radiative transition  $1s2p\ ^1P_1 \rightarrow 1s^2\ ^1S_0$  following electron-impact excitation (EIE) of highly charged heliumlike ions [1]. It was found that in the nonrelativistic limit the linear polarization is independent of the atomic number  $Z$ , while it becomes strongly  $Z$  dependent when the relativistic effects are taken into account. However, as a very important part of the relativistic effects, the effect of the Breit interaction (i.e., higher-order corrections of the electron-electron interaction beyond the Coulomb interaction [2,3]) on linear polarization of the characteristic photons following the EIE of heliumlike ions, was not considered and later was never revisited.

In the past several decades, it has been well known that the Breit interaction plays very important roles in relativistic collisions of highly charged high- $Z$  ions with continuum electrons and subsequent (non)radiative decays [4–29]. For example, Fontes *et al.* calculated EIE collision strengths of heliumlike  $\text{Fe}^{24+}$  and  $\text{Xe}^{52+}$  ions at various impact energies by using the relativistic distorted-wave (RDW) theory [15]. It was found that at high impact energies the Breit interaction contributes to increasing the cross sections even by a factor of 2 for medium- $Z$   $\text{Xe}^{52+}$  ions, while its contribution reaches over 10% even for low- $Z$   $\text{Fe}^{24+}$  ions. Bostock *et al.* studied linear polarization of the Lyman  $\alpha_1$  line following EIE of hydrogenlike  $\text{Ar}^{17+}$ ,  $\text{Ti}^{21+}$ , and  $\text{Fe}^{25+}$  ions with the relativistic close-coupling method [16]. They found that inclusion of the Breit interaction can perfectly explain the existing discrepancies between the

previous theoretical [1] and experimental results [17]. In an electron-beam ion trap (EBIT) experiment, Nakamura *et al.* discovered that the Breit interaction dominates dielectronic recombination (DR) of lithiumlike ions [18]. In light of this work, Fritzsche *et al.* proposed to reveal the dominance of the Breit interaction by measuring linear polarization of the electric dipole ( $E1$ ) line  $1s2s^2p_{1/2}\ J=1 \rightarrow 1s^22s^2\ J=0$  of berylliumlike ions following resonant electron capture (REC) into initially lithiumlike ions [19]. Soon after, such a proposal was carried out, and the corresponding predictions were also verified by Hu *et al.* in the Tokyo EBIT experiments [20]. The dominance of the Breit interaction was also found in the linear polarization of the same  $E1$  line radiated following the EIE of medium- and high- $Z$  berylliumlike  $\text{Mo}^{38+}$ ,  $\text{Nd}^{56+}$ , and  $\text{Bi}^{79+}$  ions [21]. Thereafter, the effects of the Breit interaction on linear polarization of characteristic lines were studied extensively for collisions of highly charged (more-electron) ions with electrons [22–26]. Very recently, Shah *et al.* studied in both experiment and theory the linear polarization of  $K$ -shell x-ray lines following the EIE of heliumlike  $\text{S}^{14+}$  ions [30]. It was found that for such low- $Z$   $\text{S}^{14+}$  ions the Breit interaction does not change the linear polarization of the  $K$ -shell x-ray lines [30].

Apart from linear polarization of characteristic (x-ray) lines, the effect of the Breit interaction on their angular distribution was also explored, although not as extensively as the former. For instance, Fritzsche *et al.* theoretically studied the angular distribution of the  $E1$  emission line  $1s2s^2p_{1/2}\ J=1 \rightarrow 1s^22s^2\ J=0$  of highly charged berylliumlike ions following REC into lithiumlike ions [19]. It was found that the Breit interaction quantitatively makes the angular distribution less and less anisotropic with increasing atomic number  $Z$  and even qualitatively alters its angular emission pattern for higher- $Z$  ions, i.e., from a forward- and

\*zhongwen.wu@nwnu.edu.cn

backward-dominated emission pattern to a perpendicularly dominated one, which was later verified by the experiments performed at EBIT facilities [27,28]. Moreover, such quantitative and qualitative influences of the Breit interaction were also obtained for the angular distribution of the same  $E1$  line following EIE of high- $Z$  berylliumlike ions at high impact electron energies [29]. Recently, Gumberidze *et al.* studied both experimentally and theoretically the angular distribution of characteristic  $K\alpha$  radiation following  $K \rightarrow L$  excitation of heliumlike  $U^{90+}$  ions in relativistic collisions with hydrogen and argon targets [31]. They showed that the experimental data can be well described by calculations taking into account the excitations by the target nucleus as well as by the target electrons and also demonstrated that the EIE process plays an important role in the angular distribution of the  $K\alpha$  radiation, in which the generalized Breit interaction was included [31].

In the present work, we revisit a two-step ‘‘EIE plus radiative decay’’ process,

$$\varepsilon e + 1s^2 \ ^1S_0 \rightarrow 1s2p \ ^1P_1 + \varepsilon' e \rightarrow 1s^2 \ ^1S_0 + h\nu, \quad (1)$$

of heliumlike  $Ti^{20+}$ ,  $Mo^{40+}$ ,  $Ba^{54+}$ , and  $Au^{77+}$  ions due to its significance, as stated above. Special attention is paid to the effect of the Breit interaction on the angular and polarization properties of the characteristic  $E1$  line radiated in the second step of Eq. (1). To this end, we first calculate partial EIE cross sections for the excitations from the ground state  $1s^2 \ ^1S_0$  to individual substates of the excited energy level  $1s2p \ ^1P_1$  by

$$\begin{aligned} \sigma_{\varepsilon_i}(|\beta_i J_i M_i\rangle \rightarrow |\beta_f J_f M_f\rangle) &= \frac{2\pi a_0^2}{k_i^2} \sum_{l_i j_i l'_i j'_i m_{s_i} l_f j_f m_f} \sum_{J J M} i^{l_i - l'_i} [(2l_i + 1)(2l'_i + 1)]^{1/2} \exp[i(\delta_{\kappa_i(l_i j_i)} - \delta_{\kappa'_i(l'_i j'_i)})] \\ &\times \langle l_i m_{l_i}, 1/2 m_{s_i} | j_i m_i \rangle \langle l'_i m_{l'_i}, 1/2 m_{s_i} | j'_i m_i \rangle \langle J_i M_i, j_i m_i | J M \rangle \\ &\times \langle J_i M_i, j'_i m_i | J' M \rangle \langle J_f M_f, j_f m_f | J M \rangle \langle J_f M_f, j_f m_f | J' M \rangle R(\gamma_i, \gamma_f) R^*(\gamma'_i, \gamma'_f). \end{aligned} \quad (2)$$

Here, the subscripts  $i$  and  $f$  indicate the initial and final states of the various systems involved, respectively;  $1/2$ ,  $l_i$ , and  $j_i$  are the spin, orbital, and total angular momenta of the impact electrons, respectively, and  $m_{s_i}$ ,  $m_{l_i}$ , and  $m_i$  are their projections on the  $z$  axis.  $J_i$  is the total angular momentum of the initial state  $|\beta_i J_i M_i\rangle$ , and  $M_i$  is its  $z$  projection.  $J$  and  $M$  are the total angular momentum of the impact system (i.e., an impact electron plus a target ion) and its  $z$  projection, respectively.  $\kappa_i$  is the relativistic quantum number of the impact electrons, which is fully determined by  $l_i$  and  $j_i$ .  $\beta_i$  denotes all additional quantum numbers required to specify explicitly the initial state  $|\beta_i J_i M_i\rangle$  in addition to  $J_i$  and  $M_i$ .  $\gamma_i \equiv \varepsilon_i l_i j_i \beta_i J_i J M$ .  $k_i$  is the relativistic wave number of the impact electrons, which is related to the impact energy  $\varepsilon_i$  (in rydbergs) by  $k_i^2 = \varepsilon_i(1 + \alpha^2 \varepsilon_i/4)$ .  $\delta_{\kappa_i}$  is the phase factor of the incident impact electrons. Other quantum numbers and physical quantities with the subscript  $f$  have meanings similar to the ones stated above. The standard notation of the Clebsch-Gordan coefficients has been utilized.  $a_0$  is the Born radius, and  $\alpha$  is the fine-structure constant. Moreover, the EIE transition amplitudes  $R(\gamma_i, \gamma_f)$  can be formally written

using the multiconfigurational Dirac-Fock (MCDF) and RDW methods. These partial cross sections are further employed to obtain linear polarization and angular distribution of the  $E1$  line. It is found that the Breit interaction remarkably alters the angular and polarization behaviors of the characteristic  $E1$  line, especially for high- $Z$  ions and high impact energies. To be specific, it makes the  $E1$  line less polarized and anisotropic when compared to the results with only the relativistic effects included [1], which becomes more and more prominent with increasing atomic number and impact energy, respectively.

The rest of this paper is structured as follows. In the following section, the theoretical method is given in detail. In Sec. III, we discuss the effect of the Breit interaction on the angular and polarization properties of the  $E1$  line based on the results obtained. Finally, the present work is summarized briefly in Sec. IV. Atomic units are used unless specified explicitly.

## II. THEORETICAL METHOD

### A. Partial EIE cross sections

The EIE cross sections involved in the present work are calculated by using the RDW program REIE06 [32]. In the RDW theory, if the quantization ( $z$ ) axis is chosen along the motion of impact electrons, the partial cross sections for a specific EIE from an initial state  $|\beta_i J_i M_i\rangle$  to a final state  $|\beta_f J_f M_f\rangle$  of target ions are given by [33,34]

as [34]

$$R(\gamma_i, \gamma_f) = \langle \psi_{\gamma_f} | \sum_{p,q; p < q}^{N+1} \left( \frac{1}{r_{pq}} + V_{\text{Breit}} \right) | \psi_{\gamma_i} \rangle, \quad (3)$$

where  $\psi_{\gamma_i}$  and  $\psi_{\gamma_f}$  denote antisymmetric  $(N+1)$ -electron wave functions for the initial and final states of the impact system, respectively. Besides the Coulomb potential  $1/r_{pq}$ , the Breit interaction  $V_{\text{Breit}}$  is also incorporated [35],

$$\begin{aligned} V_{\text{Breit}} &= -\frac{\boldsymbol{\alpha}_p \cdot \boldsymbol{\alpha}_q}{r_{pq}} \cos(\omega_{pq} r_{pq}) \\ &+ (\boldsymbol{\alpha}_p \cdot \nabla_p)(\boldsymbol{\alpha}_q \cdot \nabla_q) \frac{\cos(\omega_{pq} r_{pq}) - 1}{\omega_{pq}^2 r_{pq}}. \end{aligned} \quad (4)$$

Here,  $\boldsymbol{\alpha}_p$  and  $\boldsymbol{\alpha}_q$  denote the Dirac matrix vectors of electrons  $p$  and  $q$ , respectively.  $\omega_{pq}$  is an angular frequency of the virtual photon exchanged between  $p$  and  $q$ .  $r_{pq}$  is the distance between the two electrons.  $\nabla_p$  is the gradient operator for the  $p$  electron.

### B. Linear polarization and angular distribution

If EIE is the only mechanism for populating the upper level of the  $E1$  emission line ( $1s2p\ ^1P_1 \rightarrow 1s^2\ ^1S_0$ ), its linear polarization can be obtained theoretically by [36]

$$P = \frac{\sigma_0 - \sigma_{\pm 1}}{\sigma_0 + \sigma_{\pm 1}}. \quad (5)$$

Here,  $\sigma_0$  and  $\sigma_{\pm 1}$  denote the partial EIE cross sections for the excitations from the ground state  $1s^2\ ^1S_0$  to individual substates  $|M_f=0\rangle$  and  $|M_f=\pm 1\rangle$  of the excited  $1s2p\ ^1P_1$  level. In experiment, the polarization can be measured by recording yields of the emitted photons that are linearly polarized parallel and perpendicular to the reaction plane, i.e.,  $P = (I_{\parallel} - I_{\perp})/(I_{\parallel} + I_{\perp})$  [36].

With respect to the angular distribution of the  $E1$  line, moreover, the angular distribution can be expressed as [37]

$$W(\theta) \propto 1 + \beta_2 P_2(\cos \theta). \quad (6)$$

In this expression,  $P_2(\cos \theta)$  is the second-order Legendre polynomial as a function of the polar angle  $\theta$  of the emitted photons, which is determined by the propagation directions of the impact electrons and emitted photons.  $\beta_2$  represents the anisotropy parameter of the  $E1$  line, which is given by

$$\beta_2(^1P_1 \rightarrow ^1S_0) = \frac{\sqrt{2}}{2} \mathcal{A}_{20}(^1P_1). \quad (7)$$

Here,  $\mathcal{A}_{20}(^1P_1)$  refers to the second-order alignment parameter of the excited  $1s2p\ ^1P_1$  level in the density matrix theory [37,38]. It characterizes a relative population of the substates of the excited level and thus is fully determined by the partial cross sections as follows:

$$\mathcal{A}_{20}(^1P_1) = \sqrt{2} \frac{\sigma_{\pm 1} - \sigma_0}{2\sigma_{\pm 1} + \sigma_0}. \quad (8)$$

Note that the angular distribution given in Eq. (6) has been normalized with respect to the total intensity of the  $E1$  line radiated, i.e.,  $W(90^\circ) = 1 - \beta_2/2$ . In experiment, it can be readily determined by measuring yields of the  $E1$  photons emitted at different polar angles for a given azimuthal angle.

### C. Calculation of EIE transition amplitudes

As seen from Eqs. (2)–(8), the calculations of linear polarization and angular distribution of the  $E1$  line need to be traced back to the ones of the EIE transition amplitudes given in Eq. (3). Since these amplitudes appear frequently in studies of EIEs of atoms or ions [39–42], here, we just present a very brief statement. In the present work, the RDW theory is adopted to calculate the EIE transition amplitudes on the basis of the wave functions and energy levels obtained using the MCDF method.

In the MCDF method, an atomic-state wave function with well-defined parity  $P$ , total angular momentum  $J$ , and its  $z$  projection  $M$  can be expressed by using configuration-state wave functions (CSFs) with the same  $PJM$  [35,43],

$$\psi_{\alpha}(PJM) = \sum_{r=1}^{n_c} c_r(\alpha) |\phi_r(PJM)\rangle. \quad (9)$$

TABLE I. Presently calculated excitation energies (eV) from the ground state  $1s^2\ ^1S_0$  to the excited energy level  $1s2p\ ^1P_1$  of heliumlike  $\text{Ti}^{20+}$ ,  $\text{Mo}^{40+}$ ,  $\text{Ba}^{54+}$ , and  $\text{Au}^{77+}$  ions, compared with results from Glowacki [45] and Drake [46]. Results are given for the cases with (B) and without (NB) the Breit interaction included.

	$\text{Ti}^{20+}$	$\text{Mo}^{40+}$	$\text{Ba}^{54+}$	$\text{Au}^{77+}$
NB (this work)	4 753.37	18 105.73	33 207.72	70 768.42
NB (Ref. [45])	4 755.27	18 105.31	33 201.35	70 729.25
B (this work)	4 749.56	18 080.16	33 146.29	70 585.22
B (Ref. [45])	4 751.71	18 080.42	33 140.77	70 547.13
B (Ref. [46])	4 749.67	18 062.32	33 093.99	70 397.67

Here,  $n_c$  is the number of CSFs used.  $c_r(\alpha)$  denotes the configuration mixing coefficients, which are representations of the atomic state  $|\psi_{\alpha}\rangle$  in the chosen basis  $\{|\phi_r\rangle\}$ . The CSFs are generated by an antisymmetrized product of a set of orthonormal orbitals and then optimized self-consistently within a basis of the Dirac-Coulomb(-Breit) Hamiltonian. This is followed further by incorporating the quantum-electrodynamical effects into the representations  $c_r(\alpha)$  of the atomic state  $|\psi_{\alpha}\rangle$  by diagonalizing the Dirac-Coulomb(-Breit) Hamiltonian matrix.

For the presently considered EIE from the ground state  $1s^2\ ^1S_0$  to the excited level  $1s2p\ ^1P_1$  and subsequent radiative decay of heliumlike ions, the configurations  $1s^2$  and  $1snl$  ( $n = 2-3$ ,  $l = s, p, d$ ) are chosen to produce the wave functions and energy levels required using the package GRASP2K [44]. The obtained wave functions and energy levels are employed further to calculate the partial EIE cross sections by employing the RDW code REIE06 [32]. In the calculations, maximal partial waves are taken to be  $\kappa = \pm 50$  in order to ensure convergence. It should be noted that all the calculations are performed twice without (NB) and with (B) the inclusion of the Breit interaction, and as a result, the effect of the Breit interaction can be extracted. To be more specific, for the NB case the Breit interaction is not included in the calculations of both the level structure and EIE cross sections, while for the case B it is considered. Moreover, as the inclusion of the Breit interaction in the level structure hardly affects EIE cross sections even for high- $Z$  ions and high impact energies [24], the results for other cases with the Breit interaction included only in either the level structure or EIE cross sections is not shown in the present work.

## III. RESULTS AND DISCUSSION

In Table I, the presently calculated excitation energies (in eV) from the ground state  $1s^2\ ^1S_0$  to the excited energy level  $1s2p\ ^1P_1$  of heliumlike  $\text{Ti}^{20+}$ ,  $\text{Mo}^{40+}$ ,  $\text{Ba}^{54+}$ , and  $\text{Au}^{77+}$  ions adopted in Ref. [1] are listed for the two cases without and with the Breit interaction included. Since the excitation energies were not provided in Ref. [1], the present results are compared with theoretical results from Glowacki [45] and Drake [46]. As seen clearly from Table I, the present excitation energies agree excellently with the results of Glowacki [45] for both cases; the maximal discrepancy is found to be just 0.06% for high- $Z$   $\text{Au}^{77+}$  ions. Even compared

TABLE II. Comparison of the present partial and total EIE cross sections with results from Ref. [15] for the excitations from the ground state  $1s^2 \ ^1S_0$  to the individual substates  $|M_f=0\rangle$  and  $|M_f=\pm 1\rangle$  of the level  $1s2p \ ^1P_1$  of heliumlike  $\text{Fe}^{24+}$  and  $\text{Xe}^{52+}$  ions for various impact electron energies (eV). Both the present (Pres.) and referenced (Ref.) results are tabulated for the cases without (NB) and with (B) the Breit interaction. Note that the referenced cross sections are obtained here by a conversion from the original collision strengths in Ref. [15].

		$\text{Fe}^{24+}$ ( $10^{-22}$ cm $^2$ )						$\text{Xe}^{52+}$ ( $10^{-23}$ cm $^2$ )							
		$\sigma_0$		$\sigma_{\pm 1}$		$\sigma_{\text{total}}$				$\sigma_0$		$\sigma_{\pm 1}$		$\sigma_{\text{total}}$	
Energy	Case	Ref.	Pres.	Ref.	Pres.	Ref.	Pres.	Energy	Case	Ref.	Pres.	Ref.	Pres.	Ref.	Pres.
7483.19	NB	2.664	2.677	0.666	0.666	3.997	4.008	32653.92	NB	0.989	0.987	0.299	0.298	1.587	1.583
	B	2.595	2.610	0.661	0.658	3.916	3.925		B	0.904	0.906	0.284	0.271	1.471	1.449
9524.06	NB	2.935	2.965	0.759	0.770	4.453	4.506	40817.40	NB	1.107	1.112	0.309	0.310	1.725	1.733
	B	2.844	2.874	0.764	0.772	4.371	4.418		B	0.995	1.006	0.310	0.299	1.616	1.604
12245.22	NB	2.958	2.995	0.849	0.864	4.656	4.723	54423.20	NB	1.157	1.163	0.332	0.334	1.820	1.831
	B	2.843	2.883	0.866	0.879	4.575	4.641		B	1.008	1.023	0.356	0.345	1.721	1.713
16326.96	NB	2.754	2.789	0.929	0.950	4.614	4.688	81634.80	NB	1.079	1.087	0.365	0.369	1.810	1.825
	B	2.616	2.652	0.963	0.981	4.542	4.615		B	0.879	0.904	0.428	0.414	1.734	1.731
27211.60	NB	2.117	2.150	0.987	1.010	4.090	4.171	136058.00	NB	0.882	0.890	0.389	0.394	1.660	1.678
	B	1.942	1.979	1.048	1.071	4.039	4.120		B	0.625	0.668	0.502	0.481	1.630	1.630

to the results from Drake [46], the relative discrepancies are very small, the maximum of which is less than 0.27%. Moreover, it is found that the excitation energies without the Breit interaction included are overestimated by 3.8, 25.6, 61.4, and 183.2 eV for the heliumlike ions considered, respectively, which is more and more prominent for higher-Z ions.

To further illustrate the reliability of the present calculations, the presently obtained partial and total EIE cross sections are compared in Table II with results from Ref. [15] for the excitations of heliumlike  $\text{Fe}^{24+}$  and  $\text{Xe}^{52+}$  ions from the ground state  $1s^2 \ ^1S_0$  to the individual magnetic substates  $|M_f=0\rangle$  and  $|M_f=\pm 1\rangle$  of the level  $1s2p \ ^1P_1$  for various impact electron energies (eV) used in Ref. [15]. Both the present and referenced results are listed for the two cases without and with the Breit interaction. It should be noted that the referenced cross sections are obtained here by a conversion from the original collision strengths in Ref. [15]. As can be seen from Table II, the present partial and total cross sections agree very well with the results from Ref. [15] for both cases. For low-Z  $\text{Fe}^{24+}$  ions, the relative discrepancy of the partial cross sections varies within 2.37% for the NB case and within 2.20% for the other case, while that of the total cross sections changes within 1.98% and 2.01% for the two cases, respectively. For medium-Z  $\text{Xe}^{52+}$  ions, moreover, the situation is very similar to the case for  $\text{Fe}^{24+}$  ions, although a larger relative discrepancy (6.88%) of the partial cross sections  $\sigma_{\pm 1}$  corresponding to the substates  $|M_f=\pm 1\rangle$  is obtained for the B case at an impact electron energy of 136.058 keV.

Figure 1 displays the presently calculated partial EIE cross sections from the ground state  $1s^2 \ ^1S_0$  to the substates  $|M_f=0\rangle$  and  $|M_f=\pm 1\rangle$  of the  $1s2p \ ^1P_1$  level of heliumlike  $\text{Ti}^{20+}$  (top left panel),  $\text{Mo}^{40+}$  (top right),  $\text{Ba}^{54+}$  (bottom left), and  $\text{Au}^{77+}$  (bottom right) ions as a function of impact electron energy in units of their respective excitation thresholds as listed in Table I. Results are given for both cases, NB (blue dashed line with open symbols) and B (black line with solid symbols). It should be noted that the lowest impact energy considered here is taken to be 1.1 times the excitation

thresholds instead of 1.0 in order to avoid difficulties resulting from zero-energy scattered electrons in the latter case. Moreover, it should also be noted that the partial EIE cross sections corresponding to the substate  $|M_f=1\rangle$  are identical to

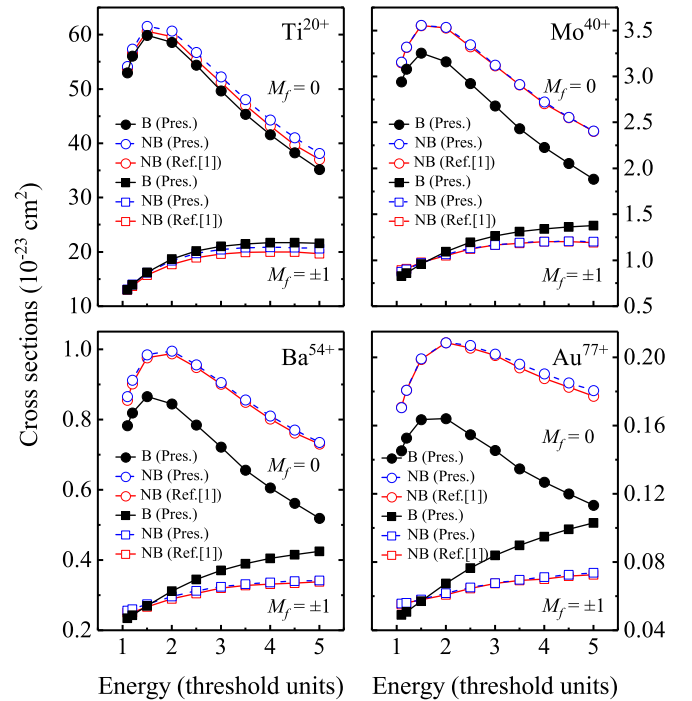


FIG. 1. Partial EIE cross sections from the ground state  $1s^2 \ ^1S_0$  to the individual substates  $|M_f=0\rangle$  and  $|M_f=\pm 1\rangle$  of the excited level  $1s2p \ ^1P_1$  of heliumlike  $\text{Ti}^{20+}$  (top left panel),  $\text{Mo}^{40+}$  (top right),  $\text{Ba}^{54+}$  (bottom left), and  $\text{Au}^{77+}$  (bottom right) ions as a function of impact electron energy in units of their respective excitation thresholds. Results are given for two cases: NB (blue dashed line with open symbols) and B (black line with solid symbols), together with the results from Reed and Chen [1] (red solid line with open symbols) for comparison.

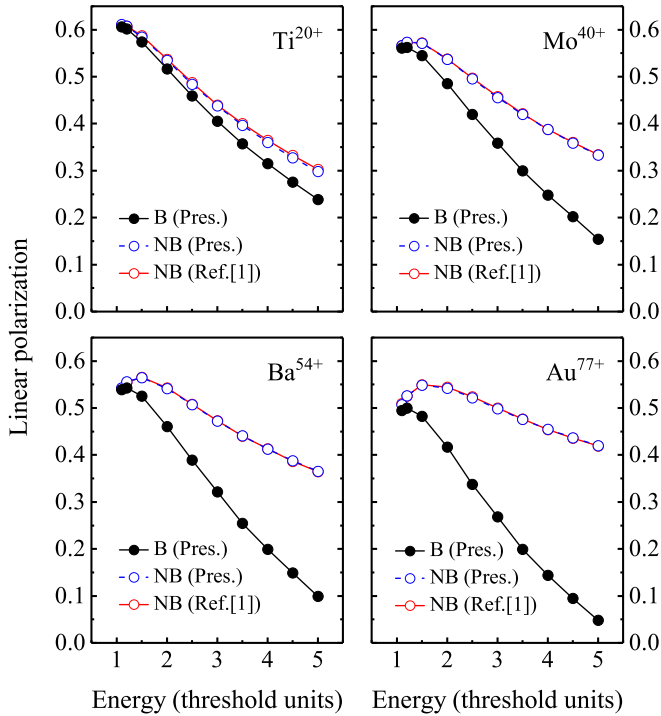


FIG. 2. Linear polarization of the characteristic  $E1$  line of heliumlike  $\text{Ti}^{20+}$  (top left panel),  $\text{Mo}^{40+}$  (top right),  $\text{Ba}^{54+}$  (bottom left), and  $\text{Au}^{77+}$  (bottom right) ions as a function of impact electron energy in the threshold units. Results are given for both cases, i.e., NB (blue dashed line with open circles) and B (black line with solid circles), along with the results of Reed and Chen [1] (red solid line with open circles) for comparison.

those corresponding to  $|M_f = -1\rangle$  due to the spatial symmetry of the EIE process considered. To illustrate the reliability of the present calculations, the results of Reed and Chen [1] (red line with open symbols) are also plotted for comparison. As seen clearly from Fig. 1, the present EIE cross sections without the inclusion of the Breit interaction agree very well with the results of Reed and Chen for all the heliumlike ions and impact energies considered. With respect to the effect of the Breit interaction, it is found that for all the heliumlike ions considered, the Breit interaction makes the partial cross sections corresponding to the substate  $|M_f = 0\rangle$  decrease at all the impact energies, while it increases those corresponding to substates  $|M_f = \pm 1\rangle$  at medium and high energies. This behavior becomes more prominent with increasing atomic number  $Z$  and impact energy. As can be inferred from Eq. (8), such an (opposite) effect of the Breit interaction on the partial EIE cross sections will alter the relative population of the energy level  $1s2p\ ^1P_1$ , which is thus expected to affect remarkably the angular and polarization behaviors of the characteristic  $E1$  line radiated in the subsequent radiative decay.

In Fig. 2, we plot the presently obtained linear polarization of the  $E1$  line radiated from the radiative decay  $1s2p\ ^1P_1 \rightarrow 1s^2\ ^1S_0$  following EIE of heliumlike  $\text{Ti}^{20+}$  (top left panel),  $\text{Mo}^{40+}$  (top right),  $\text{Ba}^{54+}$  (bottom left), and  $\text{Au}^{77+}$  (bottom right) ions as a function of impact energy in the threshold units. Again, results are shown for both cases, i.e., NB (blue dashed line with open circles) and B (black line with solid

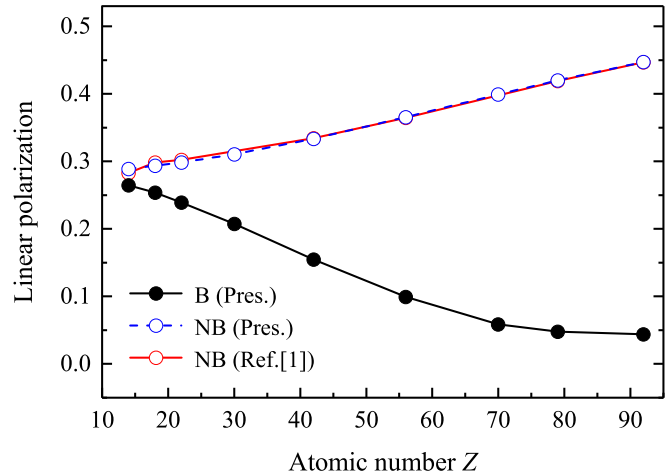


FIG. 3. Linear polarization of the  $E1$  line for an impact energy of 5.0 times the excitation thresholds as a function of the atomic number  $Z$ . Results are given for both cases, NB (blue dashed line with open circles) and B (black line with solid circles), together with the results of Reed and Chen [1] (red solid line with open circles) for comparison.

circles), along with the results of Reed and Chen [1] (red solid line with open circles) for comparison. As shown clearly, the present linear polarization without the Breit interaction included coincides very well with the results of Reed and Chen [1] for all the heliumlike ions and impact energies considered due to the very good consistency of the corresponding partial EIE cross sections obtained. Among all these results for the linear polarization, the maximal (relative) discrepancy is found to be about 1.5%, which is for low- $Z$   $\text{Ti}^{20+}$  ions at an impact energy 4.5 times the excitation threshold. As expected above, moreover, the Breit interaction remarkably alters the polarization behavior of the characteristic  $E1$  line. To be more specific, it makes the  $E1$  line very depolarized, especially for high- $Z$  ions and high impact energies. Taking high- $Z$   $\text{Au}^{77+}$  ions as an example, the absolute contribution of the Breit interaction to the linear polarization increases quickly from 0.01 to 0.37 with an increase in the impact energy from 1.1 to 5.0 times the excitation threshold.

In order to show clearly the dependence of the effect of the Breit interaction on the atomic number  $Z$ , Fig. 3 shows the linear polarization of the  $E1$  line of nine different heliumlike ions for an impact energy 5.0 times the respective excitation thresholds as a function of the atomic number  $Z$ . Results are given for both the NB (blue dashed line with open circles) and B (black line with solid circles) cases, together with the results of Reed and Chen [1] (red solid line with open circles) for comparison. Also, very good agreement between the present results and those of Reed and Chen is obtained for all the heliumlike ions considered. It is found that for the two cases the  $Z$  dependences of the linear polarization are rather different. To be specific, in the case without the Breit interaction the linear polarization increases stably from 0.29 for  $\text{Si}^{12+}$  ions to 0.45 for  $\text{U}^{90+}$  ions with increasing atomic number  $Z$ , while it decreases quickly from 0.26 to 0.04 with increasing  $Z$  after the Breit interaction is taken into consideration. Such rather different  $Z$  dependences also reveal the dominance of the Breit

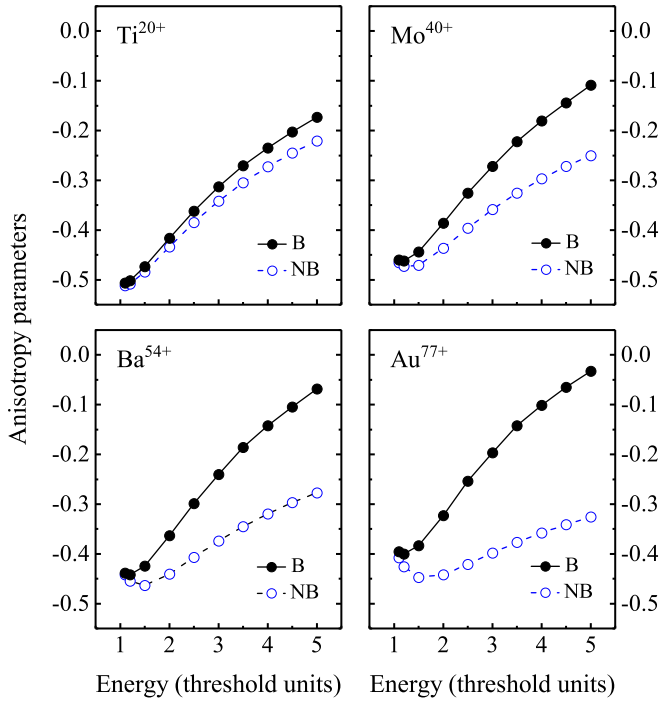


FIG. 4. Anisotropy parameters  $\beta_2$  of the characteristic  $E1$  line of heliumlike  $\text{Ti}^{20+}$  (top left panel),  $\text{Mo}^{40+}$  (top right),  $\text{Ba}^{54+}$  (bottom left), and  $\text{Au}^{77+}$  (bottom right) ions as a function of impact energy in the threshold units. Results are given for both cases, NB (blue dashed line with open circles) and B (black line with solid circles).

interaction in the linear polarization of the  $E1$  line radiated from high- $Z$  ions.

In addition to the polarization properties of the characteristic  $E1$  line radiated following EIE of heliumlike ions, as investigated by Reed and Chen [1], we explore the effect of the Breit interaction on its angular emission behaviors. As seen from Eqs. (6)–(8), the angular distribution of the characteristic  $E1$  line can be readily obtained with the use of the partial EIE cross sections. In Fig. 4, we display the presently calculated anisotropy parameters  $\beta_2$  for heliumlike  $\text{Ti}^{20+}$  (top left panel),  $\text{Mo}^{40+}$  (top right),  $\text{Ba}^{54+}$  (bottom left), and  $\text{Au}^{77+}$  (bottom right) ions as a function of the impact electron energy, which fully determines the corresponding angular distribution of the  $E1$  line. Once again, results are given for both cases for comparison, i.e., NB (blue dashed line with open circles) and B (black line with solid circles). It is found that for both cases the  $E1$  line behaves less and less anisotropically with increasing impact energy for all the heliumlike ions considered. Moreover, in comparison to the results without the Breit interaction included, the Breit interaction contributes to lowering the anisotropy of the  $E1$  line at all the impact energies considered, which becomes more and more prominent with increasing impact energy, especially for higher- $Z$  ions. Take high- $Z$   $\text{Au}^{77+}$  ions, for example; the absolute contribution of the Breit interaction to the anisotropy parameters of the  $E1$  line changes from 0.01 to 0.29 with increasing the impact energy from 1.1 to 5.0 times the excitation threshold. Furthermore, taking an impact energy 4.0 times the excitation thresholds for an example, the relative contribution of the Breit interaction to the anisotropy parameters increases

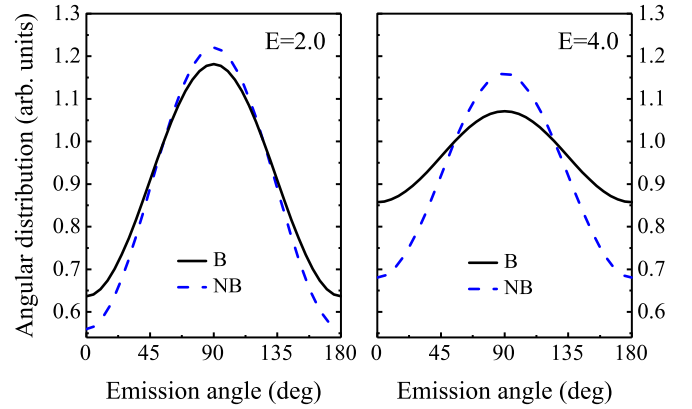


FIG. 5. Angular distribution of the  $E1$  line radiated from  $\text{Ba}^{54+}$  ions for the two cases, NB (blue dashed line) and B (black solid line). Results are presented for two different impact electron energies: 2.0 (left panel) and 4.0 (right panel) times the excitation thresholds.

quickly from 14.0% to 71.8% with increasing the atomic number from  $\text{Ti}^{20+}$  ions to  $\text{Au}^{77+}$  ions.

To illustrate the effect of the Breit interaction on the angular emission behaviors more intuitively, as an example, Fig. 5 displays the angular distribution of the  $E1$  line of  $\text{Ba}^{54+}$  ions for two different impact electron energies, 2.0 (left panel) and 4.0 (right panel) times the excitation thresholds. Results are presented again for both the NB (blue dashed line) and B (black line) cases. As seen from Fig. 5, the corresponding characteristic  $E1$  photons are dominantly emitted perpendicular to the impact electron beam axis  $z$  (i.e.,  $\theta = 90^\circ$ ) for both cases and the two impact energies. Nevertheless, the Breit interaction still quantitatively alters the angular emission behaviors of the  $E1$  photons, which makes the angular distribution of the characteristic  $E1$  line more isotropic for both impact energies considered, which becomes more prominent at higher impact energies.

Based on the detailed analysis of the effect of the Breit interaction on the partial EIE cross sections as well as the angular and polarization properties of the characteristic  $E1$  line, it has been found that the two-step EIE plus radiative decay process of heliumlike ions is remarkably affected by the Breit interaction, especially for high- $Z$  ions and high impact electron energies. In contrast to the results of Reed and Chen [1], the Breit interaction significantly alters the polarization (and angular emission) behaviors of the  $E1$  line radiated from medium- and high- $Z$  heliumlike ions. It is known from detailed MCDF calculations that the presently considered  $E1$  transition  $1s2p\ ^1P_1 \rightarrow 1s^2\ ^1S_0$  predominates over other transitions from fine-structure energy levels of the configuration  $1s2p$  to the ground state  $1s^2\ ^1S_0$  by at least three orders of magnitude except for  $1s2p\ ^3P_1 \rightarrow 1s^2\ ^1S_0$ . Nevertheless, the upper level of the transition  $1s2p\ ^3P_1 \rightarrow 1s^2\ ^1S_0$  is well isolated from the energy level  $1s2p\ ^1P_1$  of interest, especially for high- $Z$  heliumlike ions (e.g., by 22.95 eV for  $\text{Ti}^{20+}$  ions and even 2179.72 eV for  $\text{Au}^{77+}$  ions). For this reason, the presently considered two-step EIE plus radiative decay process of (medium- and high- $Z$ ) heliumlike ions is a very “clean” process, which can be proposed for use in experiment to probe the prominent effect of the Breit

interaction on the linear polarization and angular distribution of the characteristic  $E1$  line. The proposed experiment is feasible using present-day experimental facilities, such as EBITs and heavy-ion storage rings [20,47].

#### IV. SUMMARY

To summarize, in light of the work of Reed and Chen [1], the EIE and subsequent  $1s2p\ ^1P_1 \rightarrow 1s^2\ ^1S_0$  radiative decay of heliumlike ions were revisited using the MCDF method and RDW theory. Special attention was paid to the effect of the Breit interaction on the linear polarization and angular distribution of the characteristic  $E1$  line radiated from heliumlike ions. To this aim, we first calculated the partial EIE cross sections from the ground state  $1s^2\ ^1S_0$  to the individual substates  $|M_f=0\rangle$  and  $|M_f=\pm 1\rangle$  of the  $1s2p\ ^1P_1$  level. It was found that the present partial EIE cross sections without the Breit interaction agree very well with the results of Reed and Chen [1] for all the heliumlike ions and impact energies considered. The Breit interaction makes the partial cross sections corresponding to the substate  $|M_f=0\rangle$  decrease at all the impact energies, while it increases the partial ones corresponding to the  $|M_f=\pm 1\rangle$  substates at medium and high energies, which becomes more prominent with increasing atomic number and impact energy. By using these partial EIE cross sections, the linear polarization and angular distribution of the  $E1$  line were further obtained. Again, the presently obtained linear

polarization without the Breit interaction agrees very well with the results of Reed and Chen [1] for all the heliumlike ions and impact energies considered. In contrast to the results of Reed and Chen, it was found that the Breit interaction makes the characteristic  $E1$  line much less linearly polarized and anisotropic, which quickly becomes more and more prominent with increasing atomic number and impact energy. Since the presently considered  $E1$  transition  $1s2p\ ^1P_1 \rightarrow 1s^2\ ^1S_0$  is well “isolated” from other neighboring transitions in the aspects of their upper levels and/or transition rates, the two-step process of (medium- and high- $Z$ ) heliumlike ions can be proposed for use in experiment to probe the prominent effect of the Breit interaction on the angular and polarization behaviors of the  $E1$  line.

#### ACKNOWLEDGMENTS

This work has been funded by the National Key R&D Program of China under Grant No. 2017YFA0402300. Z.W.W. thanks the National Natural Science Foundation of China for Grants No. 11804280 and No. 12174315, the Longyuan Youth Innovation and Entrepreneurship Talent Project of Gansu Province of China, the Youth Science and Technology Talent Promotion Project of Gansu Provincial Science and Technology Association of China for Grant No. GXH2020626-09, and the Major Program of the Research Ability Promotion Project for Young Scholars of Northwest Normal University of China for Grant No. NWNLU-LKQN2019-5.

- 
- [1] K. J. Reed and M. H. Chen, *Phys. Rev. A* **48**, 3644 (1993).  
 [2] G. Breit, *Phys. Rev.* **34**, 553 (1929).  
 [3] G. Breit, *Phys. Rev.* **36**, 383 (1930).  
 [4] M. H. Chen and B. Crasemann, *Phys. Rev. A* **35**, 4579 (1987).  
 [5] V. I. Korobov, *Phys. Rev. A* **67**, 062501 (2003).  
 [6] D. Bernhardt, C. Brandau, Z. Harman, C. Kozhuharov, A. Müller, W. Scheid, S. Schippers, E. W. Schmidt, D. Yu, A. N. Artemyev *et al.*, *Phys. Rev. A* **83**, 020701(R) (2011).  
 [7] A. Gumberidze, D. B. Thorn, C. J. Fontes, B. Najjari, H. L. Zhang, A. Surzhykov, A. Voitkiv, S. Fritzsche, D. Banas, H. Beyer *et al.*, *Phys. Rev. Lett.* **110**, 213201 (2013).  
 [8] S. Kasthurirangan, J. K. Saha, A. N. Agnihotri, S. Bhattacharyya, D. Misra, A. Kumar, P. K. Mukherjee, J. P. Santos, A. M. Costa, P. Indelicato, T. K. Mukherjee, and L. C. Tribedi, *Phys. Rev. Lett.* **111**, 243201 (2013).  
 [9] K. N. Lyashchenko and O. Y. Andreev, *Phys. Rev. A* **91**, 012511 (2015).  
 [10] E. A. Konovalova and M. G. Kozlov, *Phys. Rev. A* **92**, 042508 (2015).  
 [11] L. Natarajan, *Phys. Rev. A* **92**, 012507 (2015).  
 [12] C. Mendoza and M. A. Bautista, *Phys. Rev. Lett.* **118**, 163002 (2017).  
 [13] M. Bilal, A. V. Volotka, R. Beerwerth, and S. Fritzsche, *Phys. Rev. A* **97**, 052506 (2018).  
 [14] A. Gumberidze, D. B. Thorn, A. Surzhykov, C. J. Fontes, B. Najjari, A. Voitkiv, S. Fritzsche, D. Banas, H. F. Beyer, W. Chen *et al.*, *Phys. Rev. A* **99**, 032706 (2019).  
 [15] C. J. Fontes, H. L. Zhang, and D. H. Sampson, *Phys. Rev. A* **59**, 295 (1999).  
 [16] C. J. Bostock, D. V. Fursa, and I. Bray, *Phys. Rev. A* **80**, 052708 (2009).  
 [17] N. Nakamura, D. Kato, N. Miura, T. Nakahara, and S. Ohtani, *Phys. Rev. A* **63**, 024501 (2001).  
 [18] N. Nakamura, A. P. Kavanagh, H. Watanabe, H. A. Sakaue, Y. Li, D. Kato, F. J. Currell, and S. Ohtani, *Phys. Rev. Lett.* **100**, 073203 (2008).  
 [19] S. Fritzsche, A. Surzhykov, and T. Stöhlker, *Phys. Rev. Lett.* **103**, 113001 (2009).  
 [20] Z. Hu, X. Han, Y. Li, D. Kato, X. Tong, and N. Nakamura, *Phys. Rev. Lett.* **108**, 073002 (2012).  
 [21] Z. W. Wu, J. Jiang, and C. Z. Dong, *Phys. Rev. A* **84**, 032713 (2011).  
 [22] H. Jörg, Z. Hu, H. Bekker, M. A. Bleszenohl, D. Hollain, S. Fritzsche, A. Surzhykov, J. R. Crespo López-Urrutia, and S. Tashenov, *Phys. Rev. A* **91**, 042705 (2015).  
 [23] Z. B. Chen, C. Z. Dong, and J. Jiang, *Phys. Rev. A* **90**, 022715 (2014).  
 [24] C. Ren, Z. W. Wu, J. Jiang, L. Y. Xie, D. H. Zhang, and C. Z. Dong, *Phys. Rev. A* **98**, 012711 (2018).  
 [25] C. Shah, H. Jörg, S. Bernitt, S. Dobredey, R. Steinbrügge, C. Beilmann, P. Amaro, Z. Hu, S. Weber, S. Fritzsche, A. Surzhykov, J. R. Crespo López-Urrutia, and S. Tashenov, *Phys. Rev. A* **92**, 042702 (2015).  
 [26] N. Nakamura, *J. Phys. B* **49**, 212001 (2016).  
 [27] Z. Hu, Y. Li, X. Han, D. Kato, X. Tong, H. Watanabe, and N. Nakamura, *Phys. Rev. A* **90**, 062702 (2014).

- [28] P. Amaro, C. Shah, R. Steinbrügge, C. Beilmann, S. Bernitt, J. R. Crespo López-Urrutia, and S. Tashenov, *Phys. Rev. A* **95**, 022712 (2017).
- [29] Z. W. Wu, M. M. Zhao, C. Ren, C. Z. Dong, and J. Jiang, *Phys. Rev. A* **101**, 022701 (2020).
- [30] C. Shah, N. Hell, A. Hubbard, M. F. Gu, M. J. MacDonald, M. E. Eckart, R. L. Kelley, C. A. Kilbourne, M. A. Leutenegger, F. S. Porter, and G. V. Brown, *Astrophys. J.* **914**, 34 (2021).
- [31] A. Gumberidze, D. B. Thorn, A. Surzhykov, C. J. Fontes, D. Banaś, H. F. Beyer, W. Chen, R. E. Grisenti, S. Hagmann, R. Hess, P.-M. Hillenbrand, P. Indelicato, C. Kozhuharov, M. Lestinsky, R. Märtin, N. Petridis, R. V. Popov, R. Schuch, U. Spillmann, S. Tashenov, S. Trotsenko, A. Warczak, G. Weber, W. Wen, D. F. A. Winters, N. Winters, Z. Yin, and T. Stöhlker, *Atoms* **9**, 20 (2021).
- [32] J. Jiang, C. Z. Dong, L. Y. Xie, and J. G. Wang, *Phys. Rev. A* **78**, 022709 (2008).
- [33] H. L. Zhang, D. H. Sampson, and R. E. H. Clark, *Phys. Rev. A* **41**, 198 (1990).
- [34] Z. W. Wu, Z. Q. Tian, J. Jiang, C. Z. Dong, and S. Fritzsche, *Phys. Rev. A* **102**, 042813 (2020).
- [35] I. P. Grant, *Relativistic Quantum Theory of Atoms and Molecules: Theory and Computation* (Springer, New York, 2007).
- [36] I. C. Percival and M. J. Seaton, *Philos. Trans. R. Soc. London, Ser. A* **251**, 113 (1958).
- [37] V. V. Balashov, A. N. Grum-Grzhimailo, and N. M. Kabachnik, *Polarization and Correlation Phenomena in Atomic Collisions* (Kluwer Academic, New York, 2000).
- [38] K. Blum, *Density Matrix Theory and Applications*, 3rd ed. (Springer, Berlin, 2012).
- [39] M. K. Inal, H. L. Zhang, and D. H. Sampson, *Phys. Rev. A* **46**, 2449 (1992).
- [40] G. X. Chen, K. Kirby, N. S. Brickhouse, T. Lin, and E. Silver, *Phys. Rev. A* **79**, 062715 (2009).
- [41] S. Mahmood, S. Ali, I. Orban, S. Tashenov, E. Lindroth, and R. Schuch, *Astrophys. J.* **754**, 86 (2012).
- [42] Z. W. Wu, Z. Q. Tian, Y. H. An, and C. Z. Dong, *Astrophys. J.* **910**, 142 (2021).
- [43] J. P. Desclaux, *Comput. Phys. Commun.* **9**, 31 (1975).
- [44] P. Jönsson, X. He, C. Froese Fischer, and I. P. Grant, *Comput. Phys. Commun.* **177**, 597 (2007).
- [45] L. Głowacki, *Atom. Data Nucl. Data Tables* **133–134**, 101344 (2020).
- [46] G. W. Drake, *Can. J. Phys.* **66**, 586 (1988).
- [47] G. Weber, H. Bräuning, A. Surzhykov, C. Brandau, S. Fritzsche, S. Geyer, S. Hagmann, S. Hess, C. Kozhuharov, R. Märtin, N. Petridis, R. Reuschl, U. Spillmann, S. Trotsenko, D. F. A. Winters, and T. Stöhlker, *Phys. Rev. Lett.* **105**, 243002 (2010).